

Absorption edge of silicon from solar cell spectral response measurements

M. J. Keevers and M. A. Green^{a)}

Centre for Photovoltaic Devices and Systems, University of New South Wales, Sydney 2052, Australia

(Received 8 July 1994; accepted for publication 8 November 1994)

The optical absorption coefficient of crystalline silicon near the band edge is determined to values as low as 10^{-7} cm^{-1} by sensitive photocurrent measurements on high efficiency silicon solar cells. Structure due to three- and four-phonon assisted absorption processes is observed. Discrepancies between absorption coefficient values around 10^{-2} cm^{-1} reported in the literature are resolved. The role of disorder theory in understanding the absorption edge of crystalline semiconductors such as silicon is discussed. © 1995 American Institute of Physics.

The absorption edge of crystalline silicon has attracted renewed interest for both practical and theoretical reasons. Knowledge of the absorption coefficient over the whole solar spectral range is crucial for simulation, characterization, and development of improved solar cells.^{1,2} A recent extension of spectral response analysis to near band gap wavelengths² suggests the growing importance of these longer wavelengths to silicon cell analysis. Several approaches are under investigation with potential for improving cell response to weakly absorbed subband gap light. These include the impurity photovoltaic effect,³ the use of Ge-Si alloy,⁴ and the quantum well cell.⁵

The subgap absorption coefficient is also of fundamental importance to an understanding of optical processes in semiconductors. The widely accepted theory for absorption in indirect crystalline semiconductors is the indirect transition theory.⁶ This explains the absorption edge in terms of indirect electron transitions from valence to conduction band, with momentum-conserving phonon emission or absorption. An alternative “disorder” theory⁷ explains the edge in terms of transitions between band tails arising from the quasistatic disorder (on the time scale of optical transitions) of thermally fluctuating lattice atoms. This leads to an exponential (Urbach) absorption edge, as in amorphous semiconductors. A recent critical assessment of these two competing theories⁸ favors the indirect transition theory, but suggests a synthesis to describe thermal broadening.

To date, several experimental methods have been used to investigate the absorption edge of silicon. Sensitive transmission measurements were performed by MacFarlane *et al.*,⁶ who determined the absorption coefficient to values as low as 10^{-3} cm^{-1} . More recent measurements⁹ show good agreement,⁸ except below around 10^{-2} cm^{-1} , where the later data support the disorder theory. However, disorder theory proponents call for further measurements as a more stringent test of the theory.^{7,10}

We report sensitive subband gap photocurrent measurements on high efficiency silicon solar cells to determine the “intrinsic” band-to-band absorption coefficient of silicon, α_{e-h} , extending the approach of Anagnostopoulos and Sadasiv.¹¹ The spectral response (SR) of a solar cell is a directly measurable quantity, defined as the short-circuit current density per unit irradiance,¹² with units of A/W:

$$\text{SR} = (1 - R) \cdot \frac{\text{IQE}}{(hc/q\lambda)}, \quad (1)$$

where

$$\text{IQE} = \frac{\alpha_{e-h}}{\alpha_{\text{tot}}} \cdot a \cdot \eta_c. \quad (2)$$

$R(\lambda)$ is the cell’s hemispherical reflectance, λ is free-space wavelength, and hc/q involves only physical constants. The internal quantum efficiency (IQE) is the fraction of photons not reflected contributing to the short-circuit current; the product of the fraction of photons entering the cell volume absorbed within that volume (the absorbance, a), the fraction of those photons absorbed generating electron-hole pairs (the ratio of the band-to-band absorption coefficient to the total absorption coefficient, $\alpha_{e-h}/\alpha_{\text{tot}}$), and the probability that the carriers generated are collected by the pn -junction (the collection efficiency, η_c).

Spectral responses were measured for high efficiency PERL¹³ (passivated emitter, rear locally diffused) silicon solar cells, exhibiting essentially 100% internal quantum efficiency from 350 to 1050 nm. In this spectral range, essentially every photon entering the cell is absorbed ($a=1$), creates an electron-hole pair ($\alpha_{\text{tot}}=\alpha_{e-h}$), and contributes to the short-circuit current ($\eta_c=1$). These cells also respond well to longer wavelengths, although effects such as light absorption in the rear metal reflector here reduce a below unity. Monochromatic light was provided by a tungsten lamp, a grating monochromator, and long-pass infrared filters to reduce stray spectral light. Wavelength was calibrated to 0.5 nm accuracy, and the spectral bandwidth ranged from 2 nm at 1000 nm to 9 nm at 1450 nm to maintain adequate signal-to-noise. The test cell was mounted on a copper block, temperature controlled to better than 0.1 °C accuracy. Diffuse reflectance from the cells was measured using an integrating sphere spectrophotometer.

Figure 1(a) shows measured values of hemispherical reflectance, relative external quantum efficiency, and the resulting relative internal quantum efficiency, for wavelengths beyond 1000 nm (1 nm intervals). Photoreponse ranges over seven orders of magnitude, with measurable response at 1450 nm, corresponding to IQE of $10^{-5}\%$.

When the internal quantum efficiency is low, it is theoretically proportional to the band-to-band absorption coefficient, α_{e-h} of the cell material.¹⁴ This holds for 280 μm

^{a)}Electronic mail: m.green@unsw.edu.au

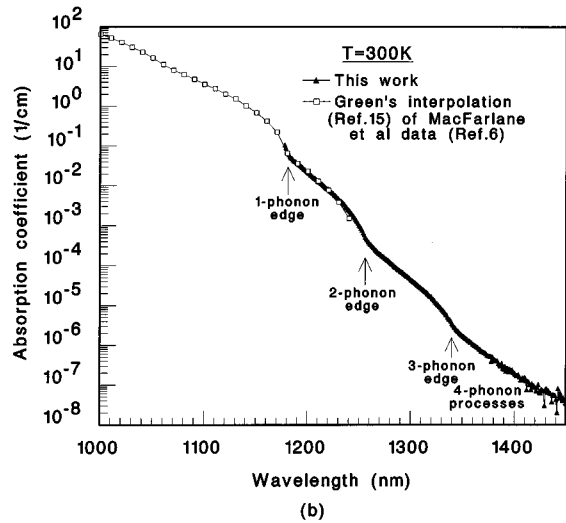
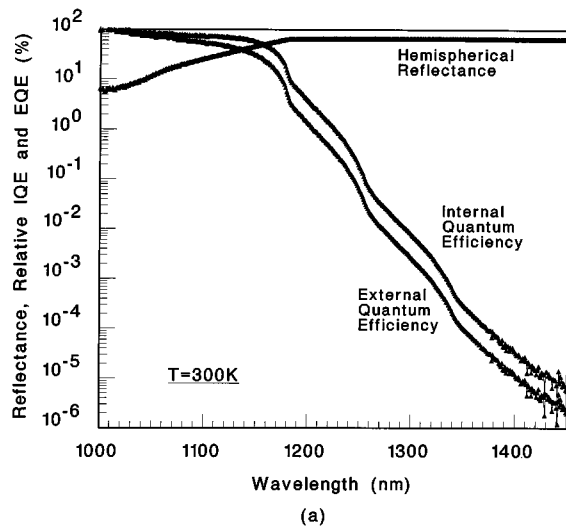


FIG. 1. (a) Internal and external quantum efficiencies, and hemispherical reflectance, of a PERL silicon solar cell. The relative IQE has been scaled to 100% at 1000 nm. (b) The absorption edge of crystalline silicon at 300 K.

thick PERL cells provided α_{tot} is less than 0.1 cm^{-1} . This allows the subgap absorption coefficient to be determined simply by scaling the IQE to an accepted value¹⁵ for the absorption coefficient at a particular wavelength (0.036 cm^{-1} at 1190 nm at 300 K, although any wavelength from 1180 to 1230 nm gives similar results). Figure 1(b) shows the resulting absorption coefficient from values around 0.1 cm^{-1} to values as low as 10^{-7} cm^{-1} , revealing structure due to three- and four-phonon assisted absorption processes. To our knowledge, this is the first direct observation of both three- and four-phonon assisted optical absorption in silicon. The unsurpassed sensitivity is partly due to the use of high performance cells, incorporating efficient light trapping. The absorption coefficient values are summarized in Table I, supplementing those tabulated by Green.¹⁵

An advantage of the photocurrent technique is that the measured response is due only to absorption creating electron-hole pairs. Other processes such as free-carrier absorption affect measurements indirectly, by diverting photons from band-to-band absorption. To investigate the possible in-

TABLE I. Absorption coefficient of crystalline silicon at 300 K (supplements tabulation of Ref. 15).

λ (nm)	α_{e-h} (cm^{-1})	λ (nm)	α_{e-h} (cm^{-1})
1190	3.6×10^{-2}	1330	8.0×10^{-6}
1200	2.2×10^{-2}	1340	3.5×10^{-6}
1210	1.3×10^{-2}	1350	1.7×10^{-6}
1220	8.2×10^{-3}	1360	41.0×10^{-6}
1230	4.7×10^{-3}	1370	6.7×10^{-7}
1240	2.4×10^{-3}	1380	4.5×10^{-7}
1250	1.0×10^{-3}	1390	2.5×10^{-7}
1260	3.6×10^{-4}	1400	2.0×10^{-7}
1270	2.0×10^{-4}	1410	1.5×10^{-7}
1280	1.2×10^{-4}	1420	8.5×10^{-8}
1290	7.1×10^{-5}	1430	7.7×10^{-8}
1300	4.5×10^{-5}	1440	4.2×10^{-8}
1310	2.7×10^{-5}	1450	3.2×10^{-8}
1320	1.6×10^{-5}		

fluence of free-carrier absorption, and also the influence of the electric field in the cell depletion region (Franz-Keldysh effect), we compared the subgap response of cells having substrates doped 1 and 100 $\Omega \text{ cm}$. No difference beyond experimental error was found. The small wavelength dependence of silicon's refractive index in the near infrared could possibly result in wavelength dependent light trapping. This would lead to different numbers of rear reflections and, hence, cell reflectivity varying with wavelength. Figure 1(a) shows R is constant with wavelength beyond 1180 nm, indicating that different light trapping modes are not encountered. Further, Fig. 1(b) shows good agreement with accepted results over their valid wavelength range. These observations lend experimental support for the theoretical proportionality between IQE and α_{e-h} .

Figure 2(a) compares the present determination of band-edge absorption at 291 and 300 K with values previously reported. Clearly, there is a discrepancy between the Cody and Brooks data⁹ and the MacFarlane *et al.* data⁶ around 10^{-2} cm^{-1} , beyond that due to temperature difference. The present measurements are in excellent agreement with the latter, bringing the accuracy of the Cody and Brooks data into question. The predictions of disorder theory,⁷ also shown, agree with the Cody and Brooks data. This has previously been used to support the disorder theory,¹⁰ although both the disorder theory and its supporting experimental evidence have been criticized.⁸ The present work demonstrates further that this supporting experimental evidence is doubtful.

Corkish and Green⁸ use photoluminescence data and detailed balance principles to predict the absorption edge. Present measurements are compared to their prediction in Fig. 2(b). The location of the three-, two-, and one-phonon edges are in agreement; however, the measured edges have a less distinct shape. This could possibly be explained by broadening due to band gap reduction in heavily doped regions of the cell (although minimized in PERL cells) or by thermal broadening. Corkish and Green⁸ suggest the possible synthesis of indirect transition and disorder theories, with the basic shape of the absorption edge described by the former,

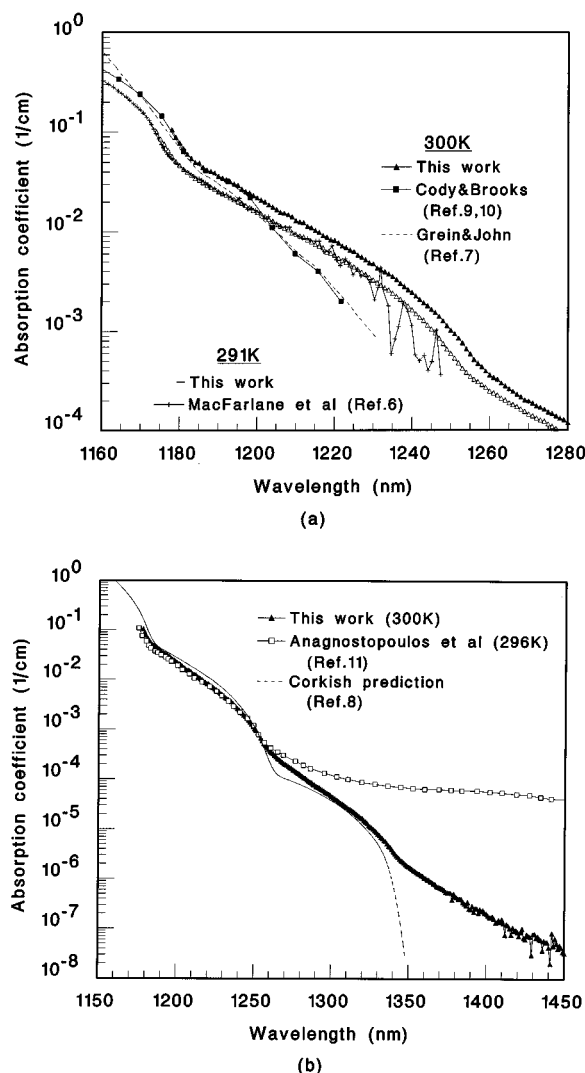


FIG. 2. (a) Comparison of the present determination of the absorption coefficient at 291 and 300 K with those of MacFarlane *et al.* (Ref. 6) and Cody and Brooks (Ref. 9). (b) Comparison of the present results with predictions based on the indirect transition theory (Ref. 8), and with earlier photocurrent measurements (Ref. 11).

and thermal broadening described by the latter. Figure 2(b) qualitatively supports their suggestion, and provides motivation for pursuing this integration.

Figure 2(b) includes the data of Anagnostopoulos *et al.*¹¹ similarly obtained from photocurrent measurements. The divergence between their data and the present at long wavelengths is most likely due to deep impurities in their devices. This reveals the usefulness of the present determination as a

base line against which to compare the response of devices, particularly those designed to extend infrared response by techniques such as the impurity photovoltaic effect.³

In conclusion, we have investigated the absorption edge of silicon by sensitive photocurrent measurements on high performance silicon solar cells, with three- and four-phonon assisted absorption processes observed. This work contributes to our understanding of band-to-band absorption by resolving a discrepancy in previously reported values of silicon's absorption coefficient. This weakens the existing case for disorder theory to play a role in the explanation of band-edge absorption. On the other hand, the more sensitive determination of the absorption coefficient reveals a structure that could possibly be explained by a synthesis of the indirect transition and disorder theories.

This work is supported by the Australian Research Council. The Centre for Photovoltaic Devices and Systems is funded by the Australian Research Council's Special Research Centres Scheme and by Pacific Power. The authors thank members of the Centre for helpful discussions and technical assistance, particularly R. Corkish, and also Professor M. Gal and his group in the School of Physics.

¹For example, see K. Bücher, J. Bruns, and H. G. Wagemann, *J. Appl. Phys.* **75**, 1127 (1994).

²P. A. Basore, *Conference Record of the 23rd IEEE Photovoltaic Specialists Conference*, Louisville, KY, May 1993, IEEE Catalog No. 93CH3283-9 (IEEE, New York, 1993), p. 147.

³M. J. Keevers and M. A. Green, *J. Appl. Phys.* **75**, 4022 (1994); in Ref. 2, p. 14.

⁴S. A. Healy and M. A. Green, *Sol. Energy Mater. Sol. Cells* **28**, 273 (1992); J. M. Ruiz J. Casado, and A. Luque, *Proceedings of the 12th European Communities Photovoltaic Solar Energy Conference*, Amsterdam, April 1994 (H. S. Stephens, United Kingdom, 1994), p. 572.

⁵K. W. J. Barnham and G. Duggan, *J. Appl. Phys.* **67**, 3490 (1990); F. W. Ragay, J. H. Wolter, A. Marti, and G. L. Araújo, in Ref. 4, p. 1429.

⁶R. J. Elliot, *Phys. Rev.* **108**, 1384 (1957); G. G. MacFarlane, T. P. McLean, J. E. Quarrington, and V. Roberts, *ibid.* **111**, 1245 (1958); T. P. McLean, *Prog. Semicond.* **5**, 53 (1960).

⁷C. H. Grein and S. John, *Phys. Rev. B* **39**, 1140 (1989); *ibid.* **41**, 7641 (1990).

⁸R. Corkish and M. A. Green, *J. Appl. Phys.* **73**, 3988 (1993); R. Corkish, Ph.D. thesis, University of New South Wales, 1993.

⁹T. Tiedje, E. Yablonovitch, G. D. Cody, and B. G. Brooks, *IEEE Trans. Electron Devices* **ED-31**, 711 (1984); Tabulated by D. E. Aspnes, *Properties of Silicon* (INSPEC, IEE, London, 1988), p. 72. See also Ref. 10.

¹⁰G. D. Cody, *J. Non-Cryst. Solids* **141**, 3 (1992).

¹¹C. Anagnostopoulos and G. Sadasiv, *Phys. Rev. B* **7**, 733 (1973).

¹²ASTM Standard E1021-84, *Annual Book of ASTM Standards*, Vol. 12.02.

¹³A. Wang, J. Zhao, and M. A. Green, *Appl. Phys. Lett.* **57**, 602 (1990).

¹⁴M. J. Keevers, Ph.D. thesis, University of New South Wales (unpublished).

¹⁵M. A. Green, *High Efficiency Silicon Solar Cells* (Trans Tech Publications, Aedermannsdorf, 1987).